BRAZILIAN JOURNAL OF OCEANOGRAPHY, 60(3):283-298, 2012

A SATELLITE VIEW OF RIVERINE TURBIDITY PLUMES ON THE NE-E BRAZILIAN COASTAL ZONE

Eduardo Negri de Oliveira[1], Bastiaan Adriaan Knoppers[2], João Antônio Lorenzzetti[3], Paulo Ricardo Petter Medeiros[4], Maria Eulália Carneiro[5] and Weber Friederichs Landim de Souza[6]*

[1]Universidade Estadual do Rio de Janeiro - Departamento de Oceanografia Física
(Rua São Francisco Xavier, n. 524, Maracanã, Rio de Janeiro, RJ, Brasil)

[2]Universidade Federal Fluminense (UFF) - Departamento de Geoquímica
(Morro do Valonguinho s/n, 24020-141 Niterói, RJ, Brasil)

[3]Instituto Nacional de Pesquisas Espaciais (INPE) - Divisão de Sensoriamento Remoto
(Av. Astronautas, 1758, 12227-010 São José dos Campos, SP, Brasil)

[4]Universidade Federal de Alagoas - Laboratório Natural e Ciências do Mar
(Rua Aristeu de Andrade, 452, 57021-090 - Maceió / AL, Brasil)

[5]Petrobras SA - Monitoramento e Avaliação Ambiental
(Av. Horácio de Macedo, 950, Ilha do Fundão, 21941-915 Rio de Janeiro, RJ, Brasil)

[6]Instituto Nacional de Tecnologia - Laboratório de Metrologia Analítica e Química
(Av. Venezuela, 82, 20081-312, Rio de Janeiro, RJ, Brasil)

*Corresponding author: negrig@gmail.com

ABSTRACT

Turbidity plumes of São Francisco, Caravelas, Doce, and Paraiba do Sul river systems, located along the NE/E Brazilian coast, are analyzed for their dispersal patterns of Total Suspended Solids (TSS) concentration using Landsat images and a logarithmic algorithm proposed by Tassan (1987) to convert satellite reflectance values to TSS. The TSS results obtained were compared to in situ collected TSS data. The analysis of the satellite image data set revealed that each river system exhibits a distinct turbidity plume dispersal pattern. The behavior, dimension and degree of turbidity of the São Francisco River plume have been greatly altered by the construction of a cascade of hydroelectric dam reservoirs in its hydrological basin. The plume has lost its typical unimodal seasonal pattern of material dispersion and its turbidity has decreased due to the regulation of river flow by the dams and TSS retainance by the reservoirs. In contrast, the Doce and Paraíba do Sul river plumes are still subject to seasonal pulsations and show more turbid conditions than the SF plume, as dams are less numerous, set in the middle river sections and the natural river flow has been maintained. The Caravelas Coastal System river plume is restricted to near shore shallow waters dominated by resuspension processes. During austral spring and summer when NE-E winds prevail, all plumes generally disperse southward. Short-term northward reversals may occur in winter with the passage of atmospheric cold fronts. The São Francisco and Doce river plumes tend to disperse obliquely to the coast and transport materials further offshore, while the Caravelas and Paraíba do Sul plumes tend to disperse mainly parallel to the coast, enhancing TSS retention nearshore.

RESUMO

O presente estudo analisa as plumas de turbidez dos sistemas dos rios São Francisco, Caravelas, Doce, e Paraiba do Sul localizados na costa NE/E do Brasil utilizando imagens Landsat e o algoritmo logarítmico para Total de Sólidos em Suspensão (TSS) proposto por Tassan (1987). Os resultados obtidos foram comparados com Total de Sólidos em Suspensão medidos in situ. A pluma de turbidez de cada sistema mostra padrões de dispersão distintos. O comportamento, a dimensão e o grau de turbidez da pluma do Rio São Francisco têm sido drasticamente alterados devido à cascata de barragens e seus reservatórios presentes em sua bacia de drenagem. Já as plumas dos rios Doce e Paraíba do Sul apresentam pulsações sazonais e maior turbidez, uma vez que as barragens nesses rios localizam-se no setor médio e mantiveram a pulsação sazonal da vazão. A pluma do sistema costeiro de caravelas permanece restrita às águas rasas dominadas por processos de ressuspensão. Durante a primavera e verão, quando os ventos de NE-E prevalecem, as plumas dos quatro sistemas se dispersam na direção sul. Durante o inverno, inversões do padrão de dispersão podem ocorrer com a passagem de frentes frias. As plumas dos sistemas São Francisco e Doce tendem a se dispersar obliquamente à costa, favorecendo o transporte de material para regiões oceânicas, enquanto que as plumas dos sistemas Caravelas e Paraíba do Sul se dispersam paralelamente à costa, favorecendo a retenção de TSS.

Descriptors: Remote sensing, Landsat, Turbidity plumes, Suspended sediments, River systems, NE-E Brazil.
Descritores: Sensoriamento remoto, Landsat, Plumas de turbidez, Sedimentos em suspensão, Sistemas fluviais, Brasil NE-E.

INTRODUCTION

The land-sea interface constitutes one of the main transport pathways of water and materials of the global hydrological and biogeochemical cycle. Rivers are responsible for the replenishment of sediments being lost by marine erosion processes along the coastal zone and the export of suspended matter and biogenic elements essential for the nourishment of coastal ecosystems (SMITH; HITCHCOCK, 1994; RAYMOND; COLE, 2003). One of the final processes of material transport along the land-sea interface occurs via coastal plumes which disperse from the river mouths onto the continental shelves (WRIGHT, 1977). Coastal plumes are also called turbidity plumes due to their higher concentration of riverine suspended matter which gives them a distinct visibility contrast against the clear oceanic waters.

The dispersion of the turbidity plume is determined by the hydrodynamic and morphological characteristics inherent to the coastal zone (WRIGHT; NITTROUER, 1995). The magnitude and pulsation of river outflow, the tidal currents, the winds and the wave regime, together with the geomorphological configuration of the coast and continental shelf, determine the dispersal patterns of the plumes. Field observations and numerical models have shown that the Coriolis force added to the wind drift and the resulting Ekman transport, can also play an important role in the dynamics and spatial distribution of coastal plumes (O'DONNELL, 1990, MASSE; MURTHY, 1990; MÜNCHOW; GARVIN, 1993).

The transport of matter along the plume occurs in several stages: 1) the initial deposition of higher density sediments around the river mouth, which usually includes more than 90% of river sediments, 2) dispersion, dilution, gradual sedimentation and accumulation of the finer material that outlasts the stage of initial deposition, and 3) the final export via material cascading over the bottom and of the ultra-fine suspended material at the outer perimeter of the plume (WRIGHT; NITTROUER, 1995). Material dispersal by turbidity plumes is also affected by other important processes operating in the coastal zone, such as the resuspension of bottom material in shallow areas subject to high wave and tidal energy regimes and longshore drift of matter originating from coastal erosion. Physical-chemical processes (flocculation, aggregation and desorption) and biological activities (primary production) also influence the progress of material scattered by the plume (WRIGHT; NITTROUER, 1995; DAGG et al., 2004). Sediments can, further, affect the water quality and serve as carriers and storage agents of phosphorus, nitrogen and organic contaminants (LODHI et al., 1997; GEYER et al., 2004). Turbidity plumes can also, therefore, be a potential source of pollution, fertilization and degradation of the water quality of the coastal and shelf regions (SCHIEBE et al., 1992; LODHI et al., 1997, WANG et al., 2009).

Satellite remote sensing has been successfully used for mapping suspended particle concentrations and the seasonal movements of turbid estuarine plumes (MAUL; GORDON, 1975; MOORE, 1980; DEKKER et al., 2002; DOXARAN et al., 2006). The spatial/temporal information provided by the satellite data is also very useful in the initialization and validation of numerical hydro-sedimentary models, which can be used to quantify sedimentary fluxes and estimate the fluvial solid discharges to the ocean (SIEGEL et al., 1999; DOUILLET et al., 2001).

Several studies have used Landsat imagery to estimate suspended sediment and to describe river plume dynamics (MAUL; GORDON, 1975; MOORE, 1980; ARANUVACHAPUN; LEBLOND, 1981; BRAKEL, W.H., 1984; DINNEL et al., 1990; BRAGA et al., 1993; BABAN, 1995; HELLWEGER et al., 2004; SIRIPONG, A., 2010; MILLER et al., 2011). Their high spatial resolution (30 meters) associated with a large spatial coverage (185 km) provides a good view of the plumes and the dispersion patterns of TSS.

Starting basically in the 1970´s, an important issue involved in the quantitative usage of satellite images for coastal environmental issues has been the development of empirical algorithms to retrieve suspended sediment concentration from ocean reflectance data (RITCHIE et al. 1976; HOLYER, 1978; AMOS; ALFOLDI, 1979). More recently, several studies on this subject have appeared (KHORRAM, 1981; TASSAN, 1987; NOVO et al. 1989; MERTES et al., 1993; WARRICK et al., 2004; DOXARAN et al., 2006; DEKKER et al., 2002, OUILLON et al., 2004; WANG et al., 2009), trying to address the complex interaction of light properties (reflection, refraction, absorption and scattering) with the liquid surface, pure water, suspended sediments, dissolved substances, chlorophyll pigments, as well as dealing with the necessary correction for atmospheric effects. To the best of our knowledge, no study has yet been undertaken either to test or establish local or regional TSS satellite reflectance algorithms for the NE-E Brazilian coastal and shelf waters.

The coastal zone of this region harbors several important medium-sized river systems which generate substantial turbidity plumes. These include the São Francisco, Doce and Paraíba do Sul rivers and also the Caravelas Coastal System, which consists of several small rivers. Each of these systems is characterized by a different typology and nature of anthropogenic impact on its drainage basin. Several studies have addressed relevant issues related to the plume dispersal of the São Francisco river. River water outflow and TSS load, and its fate beyond the

São Francisco's mouth, have been addressed by MILLIMAN (1975), SOUZA and KNOPPERS (2003), KNOPPERS et al. (2006), MEDEIROS et al. (2007) and MEDEIROS et al. (2011). The Quaternary evolution, sediment deposition, transport and erosion processes, as well as the local and regional wave climate, of the São Francisco river coastal zone, Caravelas Coastal System and the Doce river mouths have been studied by DOMINGUEZ and BITTENCOURT (1996), BITTENCOURT et al. (2000 and 2007b) and BITTENCOURT et al. (2007a). Local and regional scale studies on the physical regime (water masses, currents, waves) and the alongshore and across shore transport of TSS and biogenic elements of the Caravelas Coastal System, including its estuary, have been undertaken by LEIPE et al. (1999), KNOPPERS et al. (1999), SEGAL et al. (2008) and SCHETTINI and MIRANDA, (2010). The great motivation behind these studies was the concern that the Abrolhos reefs, which belong to this region, were being threatened by land-derived sediment insilting. A re-analysis of the Brazilian offshore wave regime using modeling output covering the entire study area has been presented by PIANCA et al. (2010).

The purpose of the present study was to make use of satellite remote sensing techniques to obtain an insight into the dispersal patterns of turbidity plumes and their export potential regarding suspended matter to the sea of the four river-estuarine systems (São Francisco, Caravelas, Doce and Paraiba do Sul) of the NE-E Brazilian coast.

Study Area

The study area is located on the northeast-east coast of Brazil (Fig. 1), a region extending from the São Francisco River mouth (10.3^{o}S) to Cabo de São Tomé (22^{o}S). Two important Brazilian drainage basins are found in this area, the São Francisco River basin itself (basin area = 0.63 x 10^{6}km^{2}) and the Eastern Atlantic Basin (basin area = 0.55 x 10^{6}km^{2}) with several sub-basins, representing, respectively, 7.5 and 6.6% of the Brazilian territory (ANA, 2010). The region includes the São Francisco River (SFR), Doce River (DR) and Paraíba do Sul River (PSR) plumes, representing the largest point sources of the Northeast and Southeast Atlantic Brazilian Basin. The Caravelas Coastal System (CCS) was chosen as being representative of an area subject to diffuse continental inputs delivered by several smaller rivers, including the Jucuruçu, Itanhém, Caravelas and Peruípe, as well as because of the ecological importance of the adjacent Abrolhos reefs.

The SFR coastal zone has been drastically altered by the construction of a series of dams in the river's middle-lower basin between the 1970s and 1990s. Its annual mean discharge of more than 3000 m3/s has suffered a decline of 35 % since then(?). Its natural seasonal pulsation has been regulated to a nearly constant flow of ~ 1800 m3/s and approximately 95 % of the river´s TSS is retained within the dam reservoirs (MEDEIROS et al., 2007). Prior to the construction of the dams, the river was turbid with mean values of TSS concentrations close to 70 g/m3 (MILLIMAN, 1975); river and estuarine conditions since then have become oligotrophic and transparent with mean values of TSS concentrations close to 5 g/m3(KNOPPERS et al., 2006; MEDEIROS et al., 2007 and 2011). The impact of the dams has thus considerably altered the estuarine processes, the fertilization potential of the coast, the downdrift and updrift transport of sediments and also drastically enhanced coastal erosion (KNOPPERS et al., 2006; BITTENCOURT et al., 2007a; MEDEIROS et al., 2011).

The Caravelas Coastal System covers the coastal zone as far as the Abrolhos reefs located 70 km offshore, which form part of the 220 km wide Abrolhos bank. The increase in the deforestation of the river watersheds, the urbanization at the coast and the tourism on the reefs themselves, have given rise to a concern that the system may be threatened by insilting and also eutrophication (KNOPPERS et al., 1999; LEIPE et al., 1999; LEÃO, 2002).

The Doce river has an annual average discharge of 900 m^{3}/s. Deforestation has, to date, been the cause of the main impact on the basin (SOUZA; KNOPPERS, 2003).

The Paraíba do Sul river has an average annual freshwater discharge of 865 m^{3}/s. Apart from the multiple anthropic impacts in its watershed, it presents some particular typological features which influence the generation of its plume. Its lower watershed, characterized by mountainous relief, harbors great potential for water and material replenishment, its river discharge exhibiting a natural seasonal unimodal pattern. Its estuary is composed of two tidal channels, a major and a minor one (CARVALHO; TORRES, 2002).

The continental shelf of the study region is generally narrow, except for the region of CCS, where with the Abrolhos Bank it reaches more than 200 km offshore (Fig. 1). The shelf circulation is strongly influenced by a western boundary current. The South Equatorial Current (SEC) impinges directly upon the shelf off SFR and, thereafter, the Brazil Current (BC) being the southern branch of the SEC bifurcation in the region, meanders southwards along the shelf and upper slope (CASTRO; MIRANDA, 1998). The coast and the continental shelf edge of the SFR and DR systems stretch in a NE-SW direction while the CCS and PSR systems present a N-S trend. The river mouths and pro-deltas of SFR, DR and PSR

are dominated by modern and relict terrigenous sediments, largely poor in organic matter (KNOPPERS et al., 2006). The region adjacent to the CCS presents sediments mostly composed of carbonates (more than 75%) from the corals and coralline algae that form the reefs of the Abrolhos region (LEÃO, 2002; LEÃO; DOMINGUEZ, 2000).

In general, the NE-E Brazilian coast is dominated by trade winds and a high wave-energy regime (DOMINGUEZ; BITTENCOURT, 1996; BITTENCOURT et al., 2007a and 2007b; PIANCA et al., 2010). The prevailing winds are easterly and northeasterly during the summer (Dec/Jan/Feb). During the winter (Jun/Jul/Aug) the passage of synoptic cold fronts enhances wind speeds and sediment transport. For the other seasons there is an alternation between these two conditions (SEGAL et al. 2008; BITTENCOURT et al.2007a). According to HAYES's (1979) classification, which divides tidal regimes into three range categories, microtides (range 0 to 200 cm), mesotides (range 200 - 400 cm) and macrotides (> 400 cm), the São Francisco and the Caravelas Coastal systems lie in a mesotidal regime whereas the Doce and Paraíba do Sul systems are subject to microtidal conditions. The geographical division between micro- and mesotides lies in the vicinity of the Abrolhos Bank (DHN, Tide Tables, Brazilian Navy; CASTRO; MIRANDA, 1998; SCHETTINI; MIRANDA, 2010). The physiographic features of the four systems, including the area of the drainage basin (A_B), river length (L), annual mean river flow (Q_R), the width of the adjacent shelf (S_w) and the range of the tidal regime (T_r) at the coast, are summarized in Table 1.

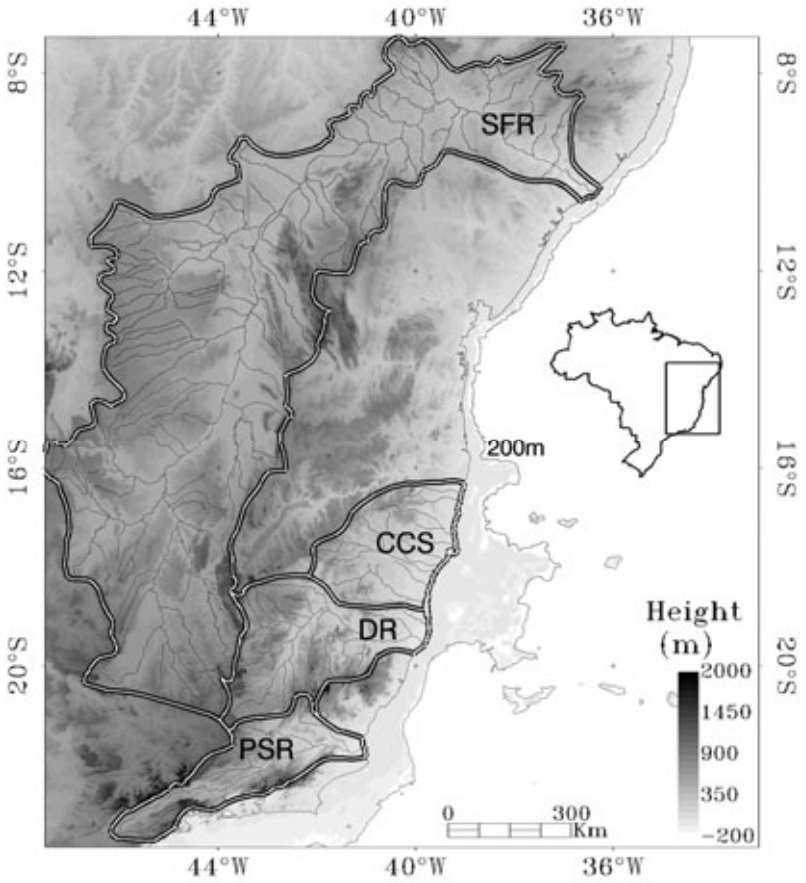

Fig. 1. São Francisco river (SFR), Caravelas Coastal System (CCS), Doce river (DR) and Paraíba do Sul river (PSR) watersheds along the Eastern Brazilian basin. Configuration from the coastline to the 200 m isobath. Adapted from: www.ana.gov.br

Table 1. Physical characteristics of SFR, CCS, DR and PSR.

River	Basin area (A_B in km^2)	River length (L in km)	River flow annual mean (Q_R in m^3/s)	Shelf width off river mouth (S_w in km)	Tidal range (T_r in cm)
SFR	622600	2700	1800	30	Mesotides, 200 to 400
CCS	65420	240	86	220	Mesotides, 200 to 400
DR	83400	853	900	40	Microtides, < 200
PSR	55500	1145	865	100	Microtides, < 200

SFR – São Francisco River, CCS – Caravelas Coastal System, DR – Doce River, PSR – Paraíba do Sul River. Sources: SOUZA; KNOPPERS, 2003; MEDEIROS et al., 2007; ANA, 2010; SCHETTINI; MIRANDA, 2010. Note: Basin area, river length and river flow of CCS correspond to the combined data of several small-sized rivers of the system.

Material and Methods

The approach used to estimate sediment dispersion patterns of each river plume system was to couple a previously established empirical algorithm for TSS estimation from visible images to an atmospheric correction model which was used to generate reflectance images from the radiance data provided by the Landsat images for each channel. Verification was carried out using TSS data sets collected in situ.

TSS insitudata, Satellite Images and Physical Setting

In situ TSS concentration was obtained during various oceanographic campaigns. The dispersion patterns of TSS in the SFR coastal zone were studied who carried out monthly field cruises from Nov/2000 to Jan/2002. TSS data of CCS, DR and PSR were obtained during oceanographic cruises aboard the R/V Victor Hensen (Leg 1 in Dec/1994 and Leg 3 in Jan/1995) within the scope of the JOPS II research program (BALZER; KNOPPERS, 1996; LEIPE et al., 1999). Additional information on TSS for PSR was obtained from LEIPE et al. (1999) who performed monthly cruises in the coastal zone between Jul/1994 and Jul/1995. Water samples from the plumes of SFR, DR and PSR were collected from ship transects set up from the river mouth along the estuarine gradient and the main axes of the plumes to their offshore limits along the shelf break. Water samples in the CCS region were collected along transects parallel to the coast and in the channels of the Abrolhos reef system (KNOPPERS et al. 1999; LEIPE et al. 1999).

For all the campaigns the TSS concentration (g/m^3) was determined gravimetrically following the procedures outlined by STRICKLAND and PARSONS (1972). A known volume of water collected at the water surface (~ 0.5 m depth) was filtered through 0.7 µm Whatman GF/F glass fiber filters. The filters were then rinsed with Milli-Q water to remove salts, dried at 60°C for four days, and reweighed on a Sartorius high precision (± 0.00001 g) balance.

Landsat-5/-7 digital satellite images of sensors Thematic Mapper (TM) and Enhanced Thematic Mapper (ETM), at a spatial resolution of 30 m were freely obtained from the National Institute for Space Research (INPE, Brazil; Landsat data base), either concomitant with or as close as possible to the days of *in situ* TSS sampling. Table 2 shows the dates of the images obtained with the associated meteorological, hydrological and oceanographic conditions (wind speed and direction, river discharge, tidal phases with their maximum and minimum heights) observed during *in situ* sampling and from Brazilian databases (River discharge from ANA; Wind from INMET<www.inmet.gov.br>) and tides from DHN Tide Tables, Brazilian Navy. In five out of the twelve cases analyzed no Landsat image was available due to heavy cloud cover in the region. For these cases, five Landsat images were obtained for the same season, month and hydrological conditions but for another year (See Table 3). Despite some fluctuations, the wind conditions observed in all the cases analyzed were typical for the respective regions and for the periods of *in situ* sampling and acquisition of Landsat images.

Table 2. Physical conditions during the dates of the Landsat images obtained.

River	Date of landsat image	Tidal stage	Minimum and maximum tidal height (cm)	Tidal height ** (cm)	Daily mean river discharge (m^3/s)	Daily mean wind speed (m/s) and direction
SFR	24/07/2000	Low tide	55/156	154	1786	6, SE
	31/12/2000	Ebb	49/156	130	1906	6, NE
	17/02/2001	Flood	68/147	107	1995	5, E
	05/09/2001	Ebb	20/178	55	1153	7, SE
CCS*	07/01/1995	Ebb	46/241	230	53	5, NE
	16/06/1995	Ebb	26/291	128	64	5, NE
DR	06/12/1994	Ebb	20/130	70	1070	7, NE
	05/08/1996	Ebb	50/120	100	306	2, E
	27/12/1996	Ebb	10/120	90	2775	6, NE
PSR	06/07/1994	Flood	30/100	60	454	4, NE
	10/10/1994	Ebb	30/100	54	364	5, NE
	13/12/1994	Flood	38/90	42	760	6, NE

SFR – São Francisco River, CCS – Caravelas Coastal System, DR – Doce River, PSR – Paraíba do Sul River. *Corresponds to the sum of the average daily discharge of the Jacuruçu, Itanhem and Peruípe Rivers (Caravelas River discharge is not included due to lack of information). **Tidal height during image acquisition.

The algorithm for satellite estimation of TSS

An analysis of various empirical models correlating TSS and remote sensing reflectance (R_{rs}) is presented by XIA (1993). This author points out that the logarithmic model works well as long as the TSS concentrations are less than 300 g/m^3. Visible bands have been successfully used to estimate TSS, particularly in less turbid waters (e.g. TSS values below 100 g/m^3). For TSS concentrations less than 50 g/m^3, as was the case of this study, a maximum R_{rs} is observed near 570nm (DEKKER et al., 2002, OUILLON et al., 2004). In addition to single band algorithms, band ratios have also been used as estimators of TSS, but some residues of atmospheric aerosol scattering may remain in the visible bands after the atmospheric correction procedure, which may interfere in the algorithm performance (WANG et al., 2009).

The following logarithmic relationship between the TSS (g/m^3) and R_{rs} can be found in several studies (KHORRAN, 1981; TASSAN, 1987; MERTES et al., 1993):

$$log(TSS) = a + b\ log\ (R_{rs}(570nm)) \quad (1)$$

where a and b are constants and $R_{rs}(570nm)$ is the Landsat Band 2 remote sensing reflectance. Tassan (1987), analyzing a data set collected inexperiments carried out in the Adriatic Sea, came up with the following equation:

$$log(TSS) = (3.08 \pm 0.27) + (1.70 \pm 0.14)\ log(R_{rs}(570nm)) \quad (2)$$

The TASSAN (1987) logarithmic algorithm (Eq. 2) was used due to its good performance in previous studies (TASSAN, 1987; XIA, 1993; MERTES et al., 1993) and good sensitivity to low TSS values, being within the range to those found in our study area.

Digital Processing of Landsat Images and Algorithm Verification

The Landsat images were initially registered to a Geographic Grid (Datum: SAD69), with an accuracy of ± 50 meters, and the satellite sensor Digital Numbers were converted into radiance values ($Wm^{-2}sr^{-1}\mu m^{-1}$) using the calibration equations given by the U.S. Geological Survey (http://landsat.usgs.gov/science_calibration.php). The 6S atmospheric correction model (VERMOTE et al., 1997) was applied to minimize atmospheric scattering and attenuation effects on the ocean radiance measured by the satellite. Finally, the images were converted to values of R_{rs} and TSS (g/m^3) values were calculated using equation 2.

The performance of the algorithm was evaluated by comparing *in situ* sampling station TSS data with mean value derived from image data for a box of 10 x 10 pixels centered at the station position. Additionally, for each image one image TSS mean value and one sampling station TSS mean value (using all points related to the image) were calculated. The comparison of *in situ* and satellite TSS values using image-wide averages was undertaken due to the lack of a match up in time between water sample collection and the passage of the satellite during some field campaigns. For example, *in situ* field data acquisitions made on 17/06/2001 and 22/08/2001 (winter period) at the mouth of SFR were compared to the Landsat

image of day 24/07/2000 (Table 3), one year before but also during the winter. Also, no consideration was given to possible alterations in the relationships between R_{rs} and TSS owing to differences in grain-size distribution, sediment color/mineralogy, or other water properties of the individual river plumes (KIRK, 1994; SYDOR; ARNONE, 1997). These *in situ*/satellite TSS comparisons should be interpreted, however, only as an indication of the accuracy of the procedure here adopted for estimation of the TSS concentration by remote sensing, at least in an image-wide average context.

Results and Discussion

Evaluation of the TSS algorithm

The image-wide mean values of satellite and *in situ* TSS for all the regions and cases analyzed are presented in Table 3 and the scatter plot of the TSS satellite and *in situ* observed cases and respective linear regression equation are depicted in Figure 3. As can be seen, the TSS algorithm (Eq. 2) yielded fairly good results (R^2= 0.89; N= 12) for the estimation of the mean TSS values. A better agreement (R^2= 0.97, N = 7) is found if only the acquisition dates when satellite images were available close or within less than two weeks from the *in situ* TSS sampling dates are used. These corresponded to 7 of the 12 total events, which are depicted in bold in Table 3. As expected, discrepancies between satellite TSS estimates and *in situ* values generally increased the greater the time lapse which occurred between image acquisition and TSS sampling (i.e. 5 of the total of 12 events addressed). In general, however, it may be concluded that in spite of some caveats regarding *in situ* sampling and image availability, the surface TSS estimates and plume turbidity gradients seem to have been well captured by the images using equation 2. The average *in situ* TSS values varied within a narrow range, from about 2 to 16 g/m^3, a pattern that was well reproduced by estimates obtained from the Landsat images, except for one scenario of the PSR system (October 1994, Table 3) when *in situ* mean TSS concentration was 42 g/m^3 while Equation 2 yielded a value of 31 g/m^3.

Table 3. Values of TSS obtained *in situ* and estimated from Landsat images.

River	Image date	In situ sampling Date	Data source		N	In situ Values Mean	TSS SD	Satellite-retrieved values Mean	TSS SD
SFR	24/07/2000	17/06 and 22/08/2001	“		28	8.45	7.09	6.51	4.62
	31/12/2000	25/01/2002	“		17	16.51	2.82	7.77	3.47
	17/02/2001	**10/02/2001**	“		6	**7.59**	6.37	**8.10**	4.94
	05/09/2001	**19/09/2001**	“		22	**14.64**	9.50	**12.60**	6.05
CCS	**07/01/1995**	**14 to 20/01/1995**	A/B		13	**2.05**	0.60	**1.85**	0.40
	16/06/1995	14 to 20/01/1995	“		13	2.05	0.60	4.30	1.11
DR	**06/12/1994**	**17 to 21/12/1994**	A		8	**11.26**	5.71	**11.35**	5.24
	05/08/1996	17 to 21/12/1994	“		8	11.26	5.71	6.78	2.00
	27/12/1996	17 to 21/12/1994	“		8	11.26	5.71	12.95	6.91
PSR	**06/07/1994**	**14/07/1994**	B/C		12	**15.41**	8.24	**14.86**	1.76
	10/10/1994	**05/10/1994**	A		12	**42.06**	38.41	**31.21**	16.14
	13/12/1994	**12 to 15/12/1994**	“		21	**12.97**	12.05	**10.19**	9.22

SFR – São Francisco River, CCS – Caravelas Coastal System, DR – Doce River, PSR – Paraíba do Sul River. N – Number of TSS *in situ* sampling stations, TSS – Total Suspended Solids, SD – Standard Deviation, both TSS and SD are expressed in g/m^3. Sources of *in situ* TSS data: A – BALZER and KNOPPERS (1996); B- LEIPE et al., 1999; C - Acquisition dates of satellite images that were close to or within less than two weeks of *in situ* TSS sampling dates are written in bold.

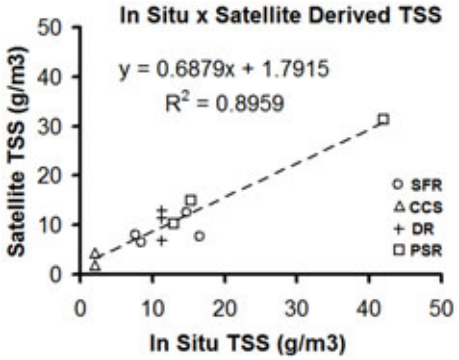

Fig. 2. Mean TSS concentrations from the data sets depicted in Table 3. SFR – São Francisco River, CCS – Caravelas Coastal System, DR – Doce River, PSR – Paraíba do Sul River.

Satellite TSS maps and ***In Situ*** TSS gradients

TSS concentration maps obtained from Landsat images and from *in situ* sampling stations for the SFR, CCS, DR and PSR systems are presented in Figures 3, 4, 5 and 6, respectively.

São Francisco River Plume:

The examples presented in Figure 3 reflect the behavior of the SFR plume conditions after the completion of the last dam constructed (Xingó), in 1994, located 180 km inland. The four examples represent the scenario of the 95% decrease in TSS river concentration in comparison to the period before the construction of the dams (MEDEIROS et al., 2007). In addition, the examples are related to a drought event that occurred in the period 2000-2001 (SOUZA; KNOPPERS, 2003). The estimated TSS concentration maps (Figs 3a,b,e,f) show four different TSS dispersal patterns. Figure 3a shows a particularly anomalous scenario exemplifying an intrusion of more turbid coastal waters, carrying resuspended matter from the pro-delta with TSS concentrations of about 14 g/m^3, into the inner and less turbid region of the estuary. This scenario occurred during neap tidal flooding and SE winds of about 6 m/s (Table 2). The composite plot (*in situ* TSS concentrations versus distance along the plume), Figure 3c, illustrates the resuspension process that was taking place in the pro-delta zone (~ 2 km off the river´s mouth) with TSS values close to 20 g/m^3.

Figure 3b exemplifies the normal post-dam conditions, with river flow of 1906 m^3/s and TSS concentration close to 5 g/m^3 (i.e. lower gray levels in the river channel).

The southern portion of the plume was less confined to the coast. The NE winds which were blowing almost parallel to the coastline at a daily average speed of about 6 m/s, favoring an offshore Ekman transport, are probably the physical agent resulting in a change in the pattern of sediment dispersal with an export of TSS to the midshelf region.

Another interesting scenario is highlighted in Figure 3e. It exhibits the presence of a feature similar to a hydraulic jetty (i.e groyne effect) (DOMINGUEZ; BITTENCOURT, 1996) produced by a river discharge of the order of 2000 m^3/s poor in TSS, reaching the pro-delta region and acting as a water barrier to the alongshore coastal drift. The adjacent regions, north and south of the river mouth, show higher TSS concentrations indicating resuspension processes and coastal erosion (KNOPPERS et al., 2006).

The plume event shown in Figure 3f illustrates a scenario that combines very low concentrations inside the river channel (5 g/m^3) and higher values in the coastal waters (25-28 g/m^3), exemplifying the relevance of resuspension processes in the region. The spring tidal currents together with the wave field generated by SE winds of about 7 m/s were likely the main forcing factors for generating a strong coastal resuspension process. In this case, wind and tidal currents were in opposite directions. Also, tides were at their greater magnitude and near to the maximum ebb tidal phase at the satellite image acquisition time (Table 2). Analyzing the Figures 3b, 3e and 3f one can see that the TSS concentrations in the river channel are lower (~ 5 g/m^3) whereas close to the coastal region the TSS concentrations are higher, clearly indicating the minor contribution of the SFR to the maintenance the turbidity plume in the region. This is particularly evident in Figures 3f and h.

As mentioned above, TSS and water flow in the SFR were reduced in their magnitude and natural seasonal variability by the operation of the dams built along the river's middle-lower course. Nevertheless, today's regulated flow is still prone to sporadic short-term perturbations induced by extreme climatic events in the drainage basin. For example, in 2004 and 2007 the SFR basin was subject to two flood events (MEDEIROS et al., 2011). The flood of 2004 was generated by high precipitation in the middle-lower semi-arid basin and yielded higher concentrations of suspended matter with a pulse of up to 490 g/m^{3}at Propriá gauging station, 40 km downstream from the dams and 80 km from the coast. The flood of 2007 produced much lower suspended matter concentrations of only up to 25 g/m^3; during this event, precipitation occurred in the upper basin and most of the suspended materials were retained by the dams (MEDEIROS et al., 2011). These two events show that the spatial variability of precipitation within the river basin may generate widely distinct TSS concentrations along both the river channel and at the coast.

Caravelas Coastal Plume

The satellite TSS fields of CCS for January (summer) and June (winter) of 1995 are displayed in Figures 4a and 4b. The only *in situ* data (Fig. 4c) for the CCS were obtained in January 1995. For both seasons, low TSS concentrations, of usually not more than 5 g/m^3 were observed in the area located on or deeper than the 10 m isobath where the coastal and outer reef arcs of the Abrolhos Bank are encountered (Fig. 4d). In contrast, higher concentrations of suspended sediments were observed between the shore and the 10 m isobath, with TSS values greater than 10 g/m^3 in the nearshore zone. We interpret these TSS dispersal patterns as a case of a river generated turbidity plume which is enhanced by bottom

resuspension processes. Materials from a number of smaller river sources (Fig. 4d) seem to be subject to mixing with resuspended matter in the nearshore zone.

The 07/01/1995 image (Fig. 4a) corresponds to an austral summer condition with a relatively low freshwater discharge from the river sources and the north-south transport of the Brazil Current (CASTRO; MIRANDA, 1998; LEIPE et al., 1999). In contrast, the 16/06/1995 image (Fig. 4b), acquired during the austral winter (under spring tide and ebbing conditions), presented a higher total river discharge of 60 m^3/s (Table 2), thus contributing to the formation of a more pronounced coastal turbidity plume with TSS concentrations of the order of 20 g/m^3. The northward trend of plume dispersal observed in Figure 4b may have been caused by the passage of a meteorological front prior to the acquisition of the image. Although winds were from E-NE when the image was recorded, SE winds associated with the frontal passage generated a reversal of the litoral drift, from southward to northward, and likely also a change in the direction of the tidal currents (LEÃO, 2002). The image obtained in winter under spring tide and ebbing conditions (Table 2) with SE-winds might indicate that larger coastal plumes are generated in the CCS in winter than in summer, when the freshwater outflow is greater. It is noteworthy that on the coast, the wet season shifts in time with respect to the interior, its peak occurring between March and May (SEGAL et al., 2008).

Studies dealing with the patterns of the current regimes, the inorganic and organic composition of TSS and the plankton assemblages of this region have revealed the presence of distinct inshore, coastal, open reef and oceanic compartments being efficiently washed-out by surface tropical waters of the southwards meandering Brazil Current at speeds of the order of 55 cm/s (LEIPE et al. 1999; KNOPPERS et al., 1999). KNOPPERS et al. (1999) show that strong alongshore currents in the inner channel between the coast and the coastal arc of the reefs (Fig. 4d) generate an efficient hydrological-geomorphological barrier to the across-shelf transport of land-derived materials upon the coastal arc and towards the outer Abrolhos reef arc, thus mitigating land-derived anthropogenic insilting.

By observing figures 4b and 4d, one can see that the CCS plumes can reach the coastal arc region during the winter season. SEGAL et al. (2008) argue that during the winter the CCS region is subject to a more dynamic physical regime, which potentially would lead to turbulent processes in the shallower nearshore waters of the continental shelf, enhancing the transport of material. Despite river runoff from the mainland, the analysis conducted by SEGAL et al. (2008) showed that the wind-driven resedimentation due to weather front activity is the major contributor to the intensification of the sedimentation processes in the offshore area of the Abrolhos reefs (outer arc region). Further, BITTENCOURT et al. (2000) demonstrated that the presence of the Abrolhos coral reefs is an important factor controlling the sediment dispersion patterns in the coastal zone, since it affords great protection against wave action. Therefore, both the hydrological-geomorphological barrier and the Abrolhos reefs seem to contribute to restricting the CCS to the coastal region.

Doce River Plume

Similarly to the SFR system, the coastline adjacent to the DR mouth lies oblique to the north-south axis. Thus, during the high water discharge in summer, the prevailing alongshore NE winds generate an offshore Ekman transport, favorable to the dispersal of the plume and TSS transport further offshore towards the 50 m isobath and the shelf edge. This can be observed on the TSS maps shown in the 06/12/1994 and 27/12/1996 images (Fig. 5a and Figure 5d, respectively). The dispersal plumes were generated under conditions of intense river discharge during the austral summer, with 1070 m3/s for the former and 2775 m^3/s for the latter case (Table 2).

The 06/12/1994 image (Fig. 5a) and the composite plot of *in situ* TSS against distance from river mouth (Fig. 5c) exhibit TSS values of about 25 g/m^3 close to the river mouth and about 10 g/m^3 at the outer limit of the plume. Close to the river mouth, SOUZA and KNOPPERS (2003) found *in situ* TSS concentrations of about 140 g/m^3during high water discharge in summer. The shallow river mouth shoals, also governed by resuspension processes, could not be accessed during *in situ* sampling (KNOPPERS et al., 1999). The continuous decline of TSS from the DR mouth towards the plume perimeter suggests that the river is the main source of TSS for the coastal plume and that processes of gradual sedimentation and dilution were operating during the dispersal.

In contrast, the image of 05/08/1996 (Fig. 5b) corresponds to a plume event during the austral winter with weak E-winds and lower river discharge (306 m3/s). The coastal region north and south of the DR mouth exhibits similar turbidity throughout the region with the lowest TSS values reaching values as low as 10 g/cm^3. The “turbidity band” was restricted to a shore-parallel band, possibly driven by the action of the E-winds.

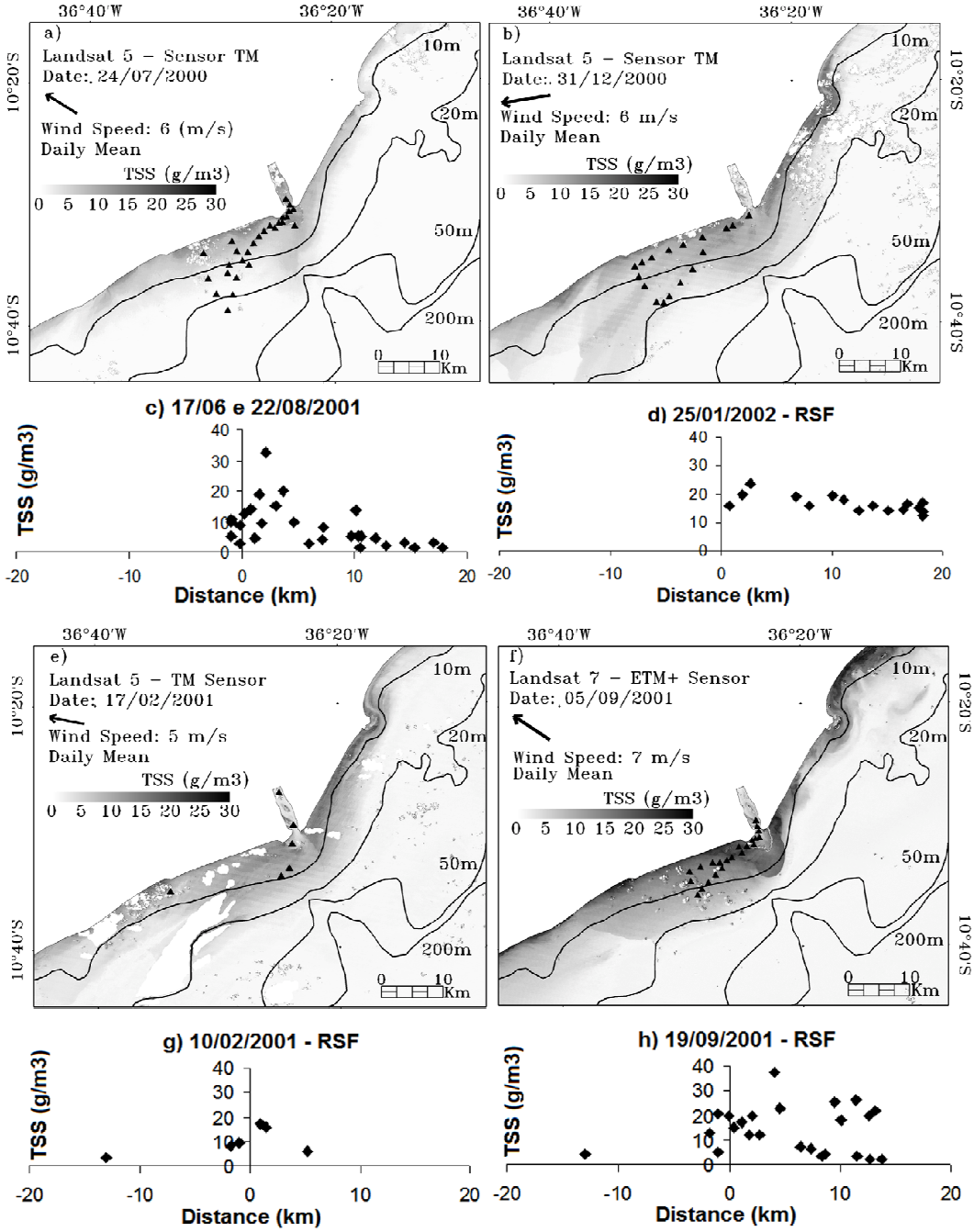

Fig. 3. São Francisco river mouth and shelf. TSS (g/m^3) estimated from Landsat images (a, b, e, f) and collected *in situ* (c, d, g, h; river mouth = 0 km). Black triangles on the images indicate the positions of *in situ* TSS stations. White areas over the water = clouds.

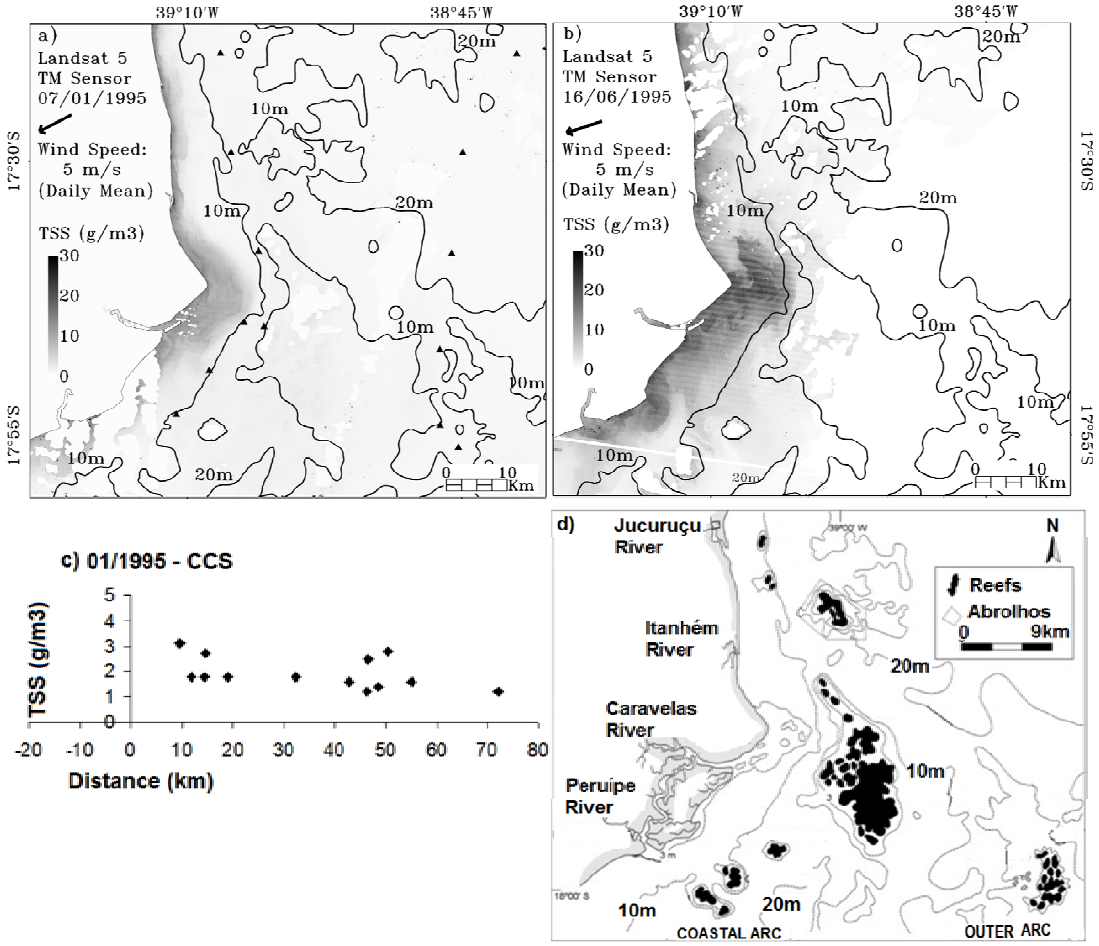

Fig. 4. The Caravelas Coastal System. Figs. 4a and b show satellite TSS (g/m^3) estimates and Figure 4c the *in situ* TSS concentrations against the distance between from shoreline and beyond the outer reef arc. Black triangles in Fig. 4a correspond to *in situ* TSS sampling stations. The Caravelas Coastal System (CCS, Figure 4d) encompassing the small-sized Jucuruçu, Itanhém, Caravelas and Peruipe rivers, the Inner Channel between the shoreline and the coastal arc, and the Abrolhos Channel between the costal arc and outer arc (adapted from LEÃO, 2002). White patches on the images correspond to clouds.

Paraíba do Sul River Plume:

Three TSS maps derived from Landsat images were chosen for the PSR river mouth. Figures 6a and b correspond to events in winter and spring, with low river discharge of 454 m^3/s and 364 m^3/s, respectively. and Figure 6e shows a summertime condition, with higher discharge (760 m^3/s). All the examples represent northeasterly wind conditions with the plumes restricted, regardless of the differences in turbidity, to a band parallel to the shore and affected by nearshore resuspension processes, as is also evidenced by the composite plots of *in situ* TSS against distance from the river mouth (Figs 6c,d,f).

Figure 6a, which represents a springtime event, shows a less well defined turbidity plume at the PSR mouth. Little sediment was transported by the river, as evidenced by the relatively low TSS concentrations (10 g/m^3). In contrast, Figure 6b, which also represents a springtime event, presents the highest suspended sediment observed in the coastal region of this study, with values as high as 40 g/m^3. Most of this suspended material is probably from bottom resuspension since the river flow transported very little suspended sediment (note that the scale bar has a range from 0 to 45 g/m^3, in order to maintain a good image contrast). Observed TSS concentrations at the PSR mouth varying from 10 to 50 g/m^3, depending on the season. As the intensity of the NE-winds was similar on both occasions, it is possible that the higher TSS concentration during the springtime plume event was generated by a swell wave field originating in distant oceanic regions.

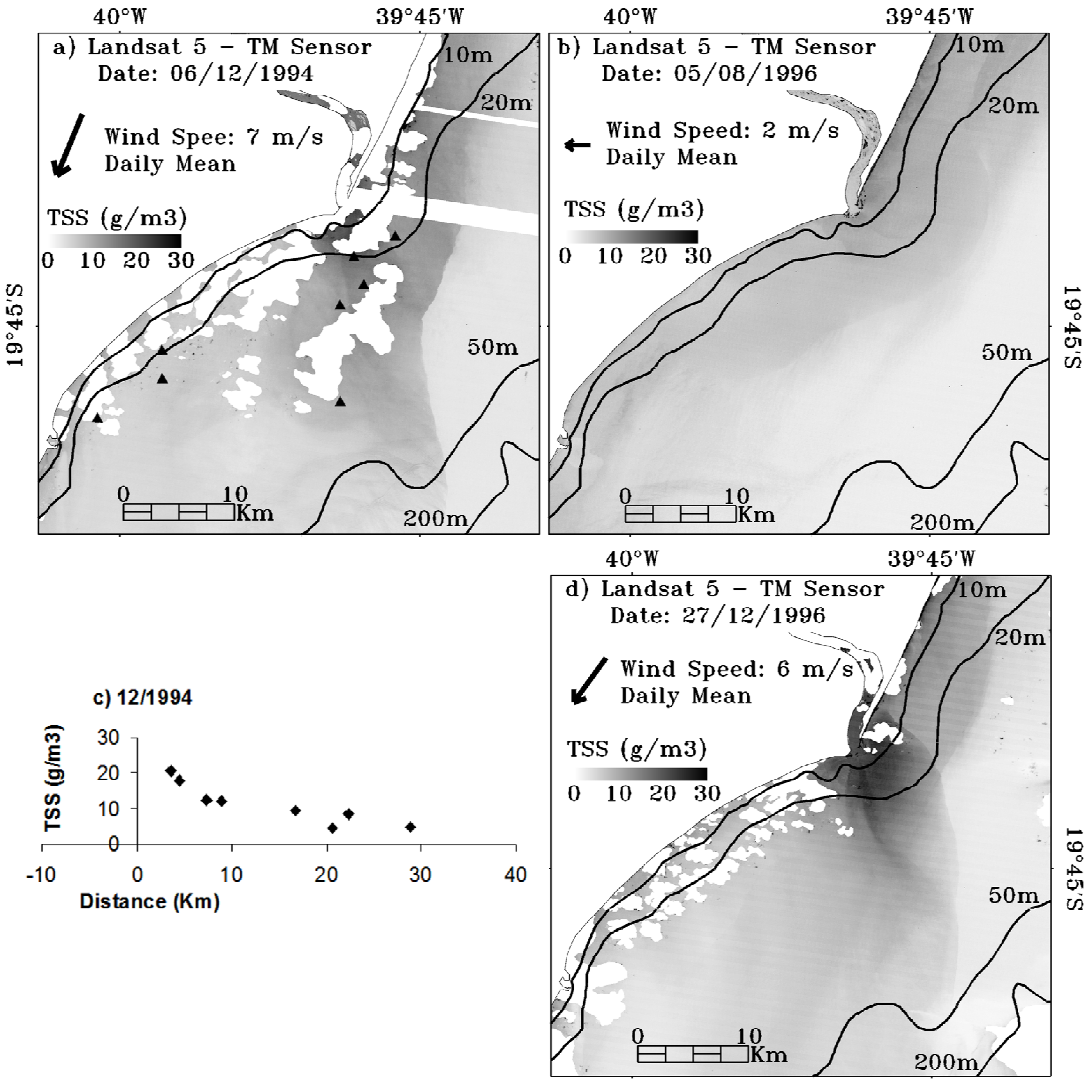

Fig. 5. The Doce river mouth and shelf system. TSS (g/m^3) estimated from Landsat images are depicted in Figures a, b, d and the acquired *in situ* TSS data plotted against the distance slightly off the river mouth in Figure 5c. Black triangles on the images indicate the positions of *in situ* TSS stations. White areas over the water correspond to clouds.

The summer event of 13/12/1994 (Fig. 6e), associated with a higher freshwater discharge (760 m^3/s), shows a river TSS concentration above 30 g/m^3 Figure 6f exhibits(?) the dispersal of a small, narrow plume extending parallel to the coast southwards from the river mouth. TSS concentrations diminished gradually due to sedimentation and dilution processes. Both estuarine channels provided the coastal zone with TSS, generating two local double lobed plumes.

The analysis of the four systems presented above shows that each system presents a distinct pattern of plume dispersal brought about by differences in river water discharge, TSS loading, anthropogenic impacts in the watersheds and particularly, also, the local topographical configuration

of the coastal zone. The study also indicates that severe alterations of land-use in the watersheds, such as engineering works (dams) and probably deforestation may greatly affect the input and also the extension of the dispersal of material upon the continental shelf. For example, BITTENCOURT et al. (2007a) pointed out that a permanent reduction in the river discharge as a result of the construction of dams, will probably have two direct consequences in the São Francisco river mouth region: (i) a chronic shoreline erosion downdrift from the mouth and (ii) a progressive deflection of the mouth in the downdrift direction. Similar processes might evolve in the Doce and Paraíba do Sul river mouths, as both are at present being subjected to the construction of dams in their lower river courses.

CONCLUSIONS

The results presented in this article show a reasonable agreement between *in situ* and estimated values of TSS concentrations obtained through the application of Tassan's 1987 algorithm. Despite the fact that no radiometric *in situ* data were available to derive a regional algorithm for TSS from satellite data, we think that the careful application of the 6S atmospheric correction model was a key element in the good performance of the algorithm. The remote sensing approach provided quantitative and synoptic views of the four river system plumes. The TSS images provided good views of the coastal sediment dispersal patterns, which would otherwise be difficult to obtain.

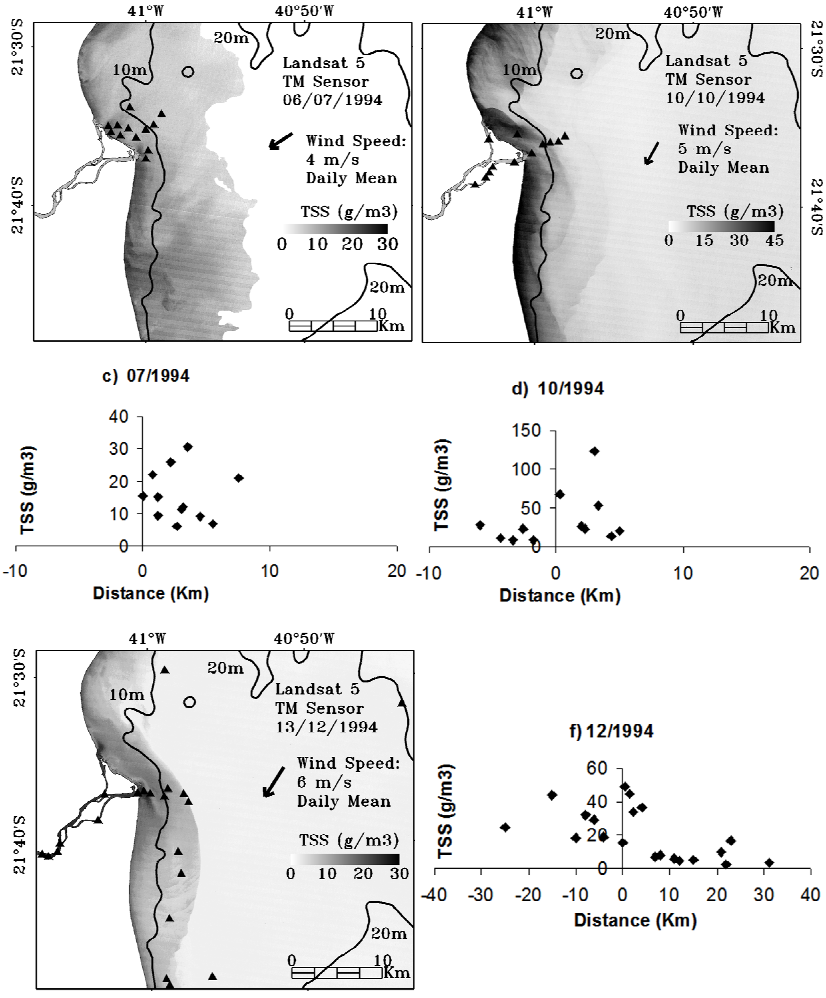

Fig. 6. Paraiba do Sul river mouth and shelf. TSS (g/m^3) estimated from Landsat images (a, b, e) and *in situ* collected (c, d, f; river mouth = 0 km). Black triangles on the images indicate the positions of TSS collected in situ. White areas over the water = clouds.

The TSS values for the river systems analyzed were, except for the Doce river in summer, generally less than 40 g/m^3. However, during periods of heavy rainfall in the drainage basin, values of TSS higher than 100 g/m^3 can be observed near the river mouths of all the four systems.

For the DR and PSR systems, the TSS concentrations carried by the river were directly related both to river discharge and to the intensity of the plume. The SFR, with its flow regulated and TSS retained by the series of dams, contributes very little to the maintenance of the turbidity plume. The plume is rather maintained by coastal resuspension processes feeding TSS from the bottom to the surface. In this case no coupling seems to occur between the river flow and the TSS concentration observed in the coastal plume.

Coastal morphology, wind regime, coastal processes and river discharge clearly determine the dispersion patterns of the sediment plumes on the eastern coast of Brazil. Although three images per river plume well short of what we consider ideal for the development of plume behavior models, the *in situ* data and the estimated satellite TSS fields suggest likely scenarios of sediment dispersion for the study region. For the SFR and DR, the coupling between the NE wind regime (frequent in summer) and the coastline orientation (NE-SW) favors an offshore Ekman transport that advects the plumes in the offshore direction onto the continental shelf. In this case the plumes can reach, or even overpass the 200 m isobath, characterizing these systems as exporters of material to the offshore oceanic region. Studies conducted on the plumes of the Columbia (THOMAS; WEATHEREBEE, 2006) and Niagara (MASSE; MURTHY, 1990) rivers also highlight the role played by Ekman transport as a source of materials to offshore regions under favorable wind conditions.

On the other hand, the CCS and the PRS plumes were oriented along the coast and kept on the inner shelf, resulting in a nearshore retention of materials. The alternation of the wind regime, and hence of waves in the coastal regions of the four systems studied, can generate reversals in the prevailing pattern of plume dispersal that generally accompany the lie of the coast.

Acknowledgments

The study was supported by the following projects: CT-Hidro/CNPq Proc.Nr. 552242/2005-5; GEF / OAS Project São Francisco, sub-project 1b-Nutrients River Estuary São Francisco and CNPq-INCT-TMOcean Proc. Nr. 573601/2008-9. B. Knoppers holds a senior CNPq scholarship (Proc. Nr. 300772/2004-1) and E.N. OLIVEIRA developed this work with a doctoral scholarship from MCT / CNPq / CT-HIDRO (Nr. 043/2004).

References

AMOS, C. L.; ALFOLDI, T. T. The determination of suspended sediment concentration in a macrotidal system using LANDSAT data. **J. Sedim. Petrol**., v. 49, p. 159-174, 1979.

ANA – Agência Nacional de Águas. Accessed: 20/08/2010 from < www.ana.gov.br>.

ARANUVACHAPUN, S.; LEBLOND, P. H. Turbidity of coastal water determined from Landsat. **Remote Sensing of Environment**, v.84, p.113-132, 1981.

BABAN, S. M. J. The use of Landsat imagery to map fluvial sediment discharge into coastal waters. **Marine Geology**, v.123, p.263–270, 1995.

BALZER, W.; KNOPPERS, B. Transport mechanisms of biogeneous material, heavy metals and organic pollutants in east Brazilian Waters, large scale investigations. In W. Ekau, & B. A. Knoppers (Eds.), **Sedimentation processes and Productivity in the Continental Shelf Waters off East and Northeast Brazil** - Joint Oceanographic Projects, Cruise Report and First Results, Leg 1, 9-25, 1996. Bremen: Center for Tropical Marine Ecology.

BITTENCOURT, A. C. S. P.; DOMINGUEZ, J. M. L.; MARTIN, L.; SILVA, I. R. Patterns of Sediment Dispersion Coastwise the State of Bahia – Brazil. **Anais da Academia Brasileira de Ciências**, v.72, n.2, p.271-287, 2000.

BITTENCOURT, A. C. S. P.; DOMINGUEZ, J. M. L.; FONTES, L. C. S.; SOUSA, D. L.; SILVA, I. R.; SILVA, F.R. Wave Refraction, River Damming, and Episodes of Severe Shoreline Erosion: The Sao Francisco River Mouth, Northeastern Brazil. **Journal of Coastal Research**, v.23, n.4, p.930-938, 2007a.

BITTENCOURT, A. C. S. P.; DOMINGUEZ, J. M. L.; MARTIN, L.; SILVA, I. R.; DE-MEDEIROS, K. O. P. Past and current sediment dispersion pattern estimates through numerical modeling of wave climate: an example of the Holocene delta of the Doce River, Espírito Santo, Brazil. **Anais da Academia Brasileira de Ciências**, v.79, n.2, p.333-341, 2007b.

BRAGA, C.Z.F.; SETZER, A.W.; LACERDA, L.D. Water quality assessment with simultaneous Landsat-5 TM data at Guanabara Bay, Rio de Janeiro, Brazil. **Remote Sensing of Environment**, v.45, n.2, p.95-106, 1993.

BRAKEL, W. H.; Seasonal dynamics of suspended-sediment plumes from the Tana and Sabaki Rivers, Kenya: Analysis of landsat imagery. **Remote Sensing of Environment**, v.16, n.2, p.165-173, 1984.

CARVALHO, C. E. V.; TORRES, J. P. M. The echohydrology of the Paraíba do Sul river, Southeast Brazil. In: McClain, M. E. (ed), **The Ecohydrology of South American Rivers and Wetlands**. The IAHS Series of Special Publications, Venice, Italy, p.179-191, 2002.

CASTRO, B. M.; MIRANDA, L. B. Physical oceanography of the western atlantic continental shelf located between 4N and 34S. In: A.R. Robinson; K.H. Brink (Ed.). **The Sea**. New York, USA: John Wiley & Sons, inc. v. 11, p. 209-251, 1998.

DAGG, M.; BENNER, R.; LOHRENZ, S.; LAWRENCE, D. Transformation of dissolved and particulate materials on continental shelves influenced by large rivers: plume processes. **Continental Shelf Research**, v. 24, p. 833-858, 2004.

DEKKER, A. G.; VOS, R. J.; PETERS, S. W. M. Analytical algorithms for lake water TSM estimation for retrospective analyses of TM and SPOT sensor data. **International Journal of Remote Sensing**, v. 23, p. 15-35, 2002.

DINNEL, S. P.; SCHROEDER, W. W.; WISEMAN, W. J. Estuarine-shelf exchange using landsat images of discharge plumes. **Journal of Coastal Research**, v. 6, n.4, p.789-799, 1990.

DOMINGUEZ, J. M. L; BITTENCOURT, A. C. S. P. Regional assessment of long-term trends of coastal erosion in Northern Brazil. **Anais da Academia Brasileira de Ciências**, v.68, p.353-371, 1996.

DOUILLET, P; OUILLON, S; CORDIER, E. A numerical model for fine suspended sediment transport in the south-west lagoon of New-Caledonia. **Corals Reefs**, v.20, p.361-372, 2001.

DOXARAN, D.; CASTAING, P.; LAVENDER, S. J. Monitoring the maximum turbidity zone and detecting fine-scale turbidity features in the Gironde estuary using high spatial resolution satellite sensor (SPOT HRV, Landsat ETM+) data. International **Journal of Remote Sensing**. v. 27, n. 11, p. 2303-2321, 2006.

GEYER, W. R.; HILL, P. S.; KINEKE, G. C.; The transport, transformation and dispersal of sediment by buoyant coastal flows. **Continental Shelf Research**, v.24, p.927-949, 2004.

HAYES, M. O. Barrier island morphology as a function of tidal and wave regime. In: Leatherman S.P. (ed.). **BarrierIslands**, Academic Press, New York, p.1-29, 1979.

HELLWEGER, F. L.; SCHLOSSER, U. L.; WEISSEL, J. K. Use of satellite imagery for water quality studies in New York Harbor. **Estuarine, Coastal and Shelf Science**, v.61, p.437-448, 2004.

HOLYER, R. J. Towards universal multispectral suspended sediment algorithms. **Remote Sensing of Environment**, v. 7, p. 323-338, 1978.

KHORRAM, S. Water quality mapping from Landsat digital data.**International Journal of Remote Sensing**. v. 2, p. 145-154, 1981.

KIRK, J. T. O. **Light and Photosynthesis in Aquatic Ecosystems**. Orlando, Florida: Academic Press, 1994. 401 p.

KNOPPERS, B.; MEYERHÖFER, M.; MARONE, E.; DUTZ, J.; LOPES, R.; LEIPE, T.; CAMARGO, R. Compartments of the pelagic system and material Exchange at the Abrolhos Bank coral reefs, Brazil. **Archive of Fishery and Marine Research**, v. 47, n.2/3, p. 285-306, 1999.

KNOPPERS, B. A.; MEDEIROS, P. R. P.; SOUZA, W. F. L.; JENNERJAHN, T. The São Francisco Estuary, Brazil. In: J. P. Wangersky (Ed.), **The Handbook of Environmental Chemistry**. Berlin-Heidelberg: Springer-Verlag, v.5, Part H, 2006, p. 51-70.

LEÃO, Z. M. A. N. Abrolhos, BA - O complexo recifal mais extenso do Atlântico Sul. *In:* Schobbenhaus,C.; Campos,D.A. ; Queiroz,E.T.; Winge,M.; Berbert-Born,M.L.C. (Eds.) **Sítios Geológicos e Paleontológicos do Brasil**. 1° ed. Brasilia: DNPM/CPRM - Comissão Brasileira de Sítios Geológicos e Paleobiológicos (SIGEP), v. 1, p. 345-359, 2002.

LEÃO, Z. M. A. N.; DOMINGUEZ, J. M. L. Tropical coast of Brazil. **Marine Pollution Bulletin**, v. 41, p. 112-122, 2000.

LEIPE. T.; KNOPPERS, B.; MARONE, E.; CAMARGO, R. Suspended matter transport in coral reef waters of the Abrolhos Bank, Brazil. **Geo- Marine Letters**, v.19, n.3, p. 186-195, 1999.

LODHI, M. A.; RUNDQUIST, D. C.; HAN, L.; KUZILA, M. The potential for remote sensing of loess soils suspended in surface waters. **Journal of American Water Resources Association**, v. 33, n.1, p.111-117, 1997.

MASSE, A. K.; MURTHY, C. R. Observations of the Niagara River thermal plume. **Journal of Geophysical Research**, v. 95, p. 851-875, 1990.

MAUL, G. A.; GORDON, H. R. On the Use of the Earth Resources Technology Satellite (LANDSAT-1) in Optical Oceanography. **Remote Sensing of Environment**, v.4, n.95, p.95-128, 1975.

MEDEIROS, P. R. P.; KNOPPERS, B. A.; SANTOS, R. C.; SOUZA, W. F. L. Aporte fluvial e dispersão de matéria particulada em suspensão na zona costeira do rio São Francisco (SE/AL). **Geochimica Brasiliensis**, v. 21, n. 2, p. 212-231, 2007.

MEDEIROS, P. R. P.; KNOPPERS, B. A.; SOUZE, W. F. L.; OLIVEIRA, E. N. Aporte de material em suspensão no baixo rio São Francisco (SE/AL) em diferentes condições hidrológicas. **Braz. J. Aquat. Sci. Technol**., v.15, n.1, p.42-53, 2011.

MERTES, L. A. K.; SMITH, M. O.; ADAMS, J. B. Estimating suspended sediment concentrations in surface waters of the Amazon river wetlands from Landsat images. **Remote Sensing Environment**, v. 43, p. 281-301, 1993.

MILLER, R. L.; LIU, C. C.; BUONASSISSI, C. J.; WU, A. M. A multi-sensor approach to examining the distribution of total suspended matter (tsm) in the albemarle-pamlico estuarine system, NC, USA. **Remote Sensing**, v.3, p. 962-974, 2011.

MILLIMAN, J. D. Upper continental margins sedimentation off Brazil: Part VI. **A synthesis. Contrib. Sedimentol**., v. 4, p.151-176, 1975.

MOORE, G. K. Satellite remote sensing of water turbidity. **Hydrological Sciences-Bulletin-des Sciences Hydrologiques**, v.25(4), n.12, p.407-421, 1980.

MÜNCHOW, A.; GARVINE, R. W. Buoyancy and wind forcing of a coastal current. **Journal of Marine Research**, v. 51, p. 293-322, 1993.

NOVO, E. M. M.; HANSOM, J. D.; CURRAN, P. J. The effect of viewing geometry and wavelength on the relationship between reflectance and suspended sediment concentration. **International Journal of Remote Sensing**, v. 10, n. 8, p. 1357-1372, 1989.

O'DONNELL, J. The formation and fate of a river plume: a numerical model. **Journal of Physical Oceanography**, v. 20, p. 551-569, 1990.

PIANCA, C; MAZZINI, P. L. F.; SIEGLE, E. Brazilian offshore wave climate based on NWW3 Reanalysis. **Brazilian Journal of Oceanography**, v.58, n.1, p.53-70, 2010.

OUILLON, S.; DOUILLET, P.; ANDREFOUET, S. Coupling satellite data with in situ measurements and numerical modeling to study fine suspended-sediment transport: a study for the lagoon of New Caledonia. **Coral Reefs**, v. 23, p. 109–122, 2004.

RAYMOND, P. A.; COLE, J. J. Increase in the export of alkalinity from North America's largest river. **Science**, v. 301, p. 88-91, 2003.

RITCHIE, J. C.; SCHIEBE, F. R.; MCHENRY, J. R. Remote sensing of suspended sediments in surface waters. **Photogrammetric Engineering and Remote Sensing**, v. 42, n.12, p. 1539-1545, 1976.

SCHETTINI, C. A. F.; MIRANDA, L. B. Circulation and suspended particulate matter transport in a tidally dominated estuary: Caravelas estuary, Bahia, Brazil. **Brazilian Journal of Oceanography**, v.58, n.1, p.1-11, 2010.

SCHIEBE, F. R.; HARRINGTON Jr., J. A.; RITCHIE, J. C. Remote sensing of suspended sediments: the Lake Chicot, Arkansas project. **International Journal of Remote Sensing**, v.13, p.1487-1509, 1992.

SEGAL, B.; EVANGELISTA, H.; KAMPEL, M.; GONÇALVES, A. C.; POLITO, P. S.; SANTOS, E. A. Potential impacts of polar fronts on sedimentation processes at Abrolhos coral reef (South-West Atlantic Ocean/Brazil). **Continental Shelf Research**, v.28, p.533-544, 2008.

SIEGEL H; GERTH, M.; MUTZKE, A. Dynamics of the Oder river plume in the Southern Baltic Sea: satellite data and numerical modelling. **Continental Shelf Research**, v.19, p.1143-1159, 1999.

SIRIPONG, A. Detect the coastline changes in Thailand by remote sensing. International Archives of the Photogrammetry, **Remote Sensing and Spatial Information Science**, Volume XXXVIII, Part 8, p.992-996, 2010.

SMITH, S. M.; HITCHCOCK, G. L. Nutrient enrichments and phytoplankton growth in the surface waters of the Louisiana bight. **Estuaries**, v. 17, p. 740-753, 1994.

SOUZA, W. F. L.; KNOPPERS, B. A. Fluxos de água e sedimentos a costa leste do Brasil: relações entre a tipologia e as pressões antrópicas. **Geochimica Brasiliensis**, v. 17, n. 1, p. 57-74, 2003.

STRICKLAND, J. D. H.; PARSONS, T. R. **A practical handbook of seawater analysis**. Ottawa: Fishery Research Board, Canada, 1972. 310p.

SYDOR, M.; ARNONE, R. A. Effect of suspended particulate and dissolved organic matter on remote sensing of coastal and riverine waters. **Applied Optics**, v. 36, n.27, p. 6905-6912, 1997.

TASSAN, S. Evaluation of the potential of the Thematic Mapper for marine application. **International Journal of Remote Sensing**, v. 8, n. 10, p. 1455-1478, 1987.

THOMAS, A. C.; WEATHEREBEE, R. A. Satellite-measured temporal variability of the Columbia River plume. **Remote Sensing of Environment**, v.100, p. 167-178, 2006.

VERMOTE, E. F.; TANRE, D.; DEUZÉ, J. L.; HERMAN, M.; MORCRETTE, J. J. Second simulation of the satellite signal in the solar spectrum, 6S: An overview. **IEEE Trans. Geosc. Remote Sens.**, v. 35, n. 3, p. 675-686, 1997.

WANG, J-J.; LU, X. X.; LIEW, S. C.; ZHOU, Y. Retrieval of suspended sediment concentrations in large turbid rivers using Landsat ETM+: an example from the Yangtze River, China. **Earth Surface Processes and Landforms**, v. 34, p. 1082-1092, 2009.

WARRICK, J. A.; MERTES, L. A. K.; SIEGEL, D. A.; MACKENZIE, C. Estimating Suspended sediment concentrations in turbid coastal waters of the Santa Barbara Channel with SeaWiFS. **International Journal of Remote Sensing**, v. 25, n. 10, p. 1995-2002, 2004.

WRIGHT, L. D. Sediment transport and deposition at river mouths: a synthesis. **Geological Society American**, v. 88, n. 6, p. 857–868, 1977.

WRIGHT, L. D.; NITTROUER, C. A. Dispersal of river sediments in coastal seas: six contrasting cases. **Estuaries**, v. 18, p. 494-508, 1995.

XIA, L. A unified model for quantitative remote sensing of suspended sediment concentration. **International Journal of Remote Sensing**, v. 14, n. 14, p. 2665-2676, 1993.

(Manuscript received 14 February 2011; revised 09 July 2012; accepted 20 July 2012)